

Direct and Parametric Entrainment of a Graphene Oscillator

Samer Hourⁱ*, Santiago J. Cartamil-Bueno*, Menno Poot*, Peter G. Steeneken*, Herre S. J. van der Zant*, and Warner J. Venstra**

*Kavli Institute of Nanoscience, Delft University of Technology, Lorentzweg 1, 2628 CJ Delft, The Netherlands

**Quantified Air, Lorentzweg 1, 2628 CJ Delft, The Netherlands

Summary. We explore the dynamics of a graphene nanomechanical oscillator coupled to an optical reference oscillator. For small detuning, the graphene oscillator phase synchronizes to the reference oscillator. Occasional phase slips occur when the detuning is increased, and for large detuning the synchronization is lost. Phase oscillations are observed in the phase-slip regime, with a frequency that exhibits a clear power-law dependence on the strength of the applied reference signal. Similar behavior occurs when the reference signal oscillates at twice the oscillator frequency, giving rise to parametric synchronization. The dynamic behavior is explained by a van der Pol-Duffing-Mathieu equation, where the Duffing parameter is shown to play a crucial role in the onset of phase oscillations. These experiments can be viewed as frequency stabilization of the fluctuating graphene oscillator by injection locking, and enable the generation of stable oscillating nanoscale motion.

Introduction

Entrainment is the phenomenon by which self-sustained oscillators mutually lock their frequencies and phase. First observed in a pair of coupled mechanical clocks by Huygens, synchronized oscillators occur in a wide variety of engineered and biological systems such as injection-locked time keeping devices, cardiac pacemaker cells and groups of fireflies [1]. In this work, entrainment of a single layer graphene (SLG) nanomechanical oscillator is explored, where the properties of the oscillator dephasing are observed as a function of the lock signal detuning and power for both direct and parametric entrainment. We focus on the systems oscillating phase and explore its dependence on the strength of the synchronization signal.

Experimental Setup

The oscillator is fabricated by transferring a single layer of chemical vapor deposition (CVD) grown graphene onto an silicon substrate with circular cavities, which are etched into a 632 nm thick thermally grown silicon oxide layer. To reduce thermal drift, the graphene drum is placed in a cryogenic chamber with optical access (Montana Instruments), and cooled down to 3 K at a pressure of $< 10^{-6}$ mbar. Figure 1(a) shows the device and the setup. To induce self-oscillations, a red He-Ne laser ($\lambda = 633$ nm) is focused on the drum. The reflection from the silicon bottom of the cavity creates a partial standing wave which introduces a position-dependent thermally-induced mechanical tension in the structure. The resulting photothermal force gradient, ∇F_{ph} , modifies the effective damping, given as $\Gamma_{\text{eff}} = \Gamma \left(1 + \frac{\omega_0}{\Gamma} \frac{\omega_0 \tau}{1 + \omega^2 \tau^2} \frac{\nabla F_{\text{ph}}}{\kappa} \right)$ where, Γ ($\Gamma = \omega_0/Q$) is the damping without feedback, ω_0 and κ are the natural frequency and spring stiffness of the graphene drum, and τ is the thermal delay time [3-5]. The measurements are performed at an incident laser power of 10 mW. The motion of the graphene drum is recorded in the time-domain by sampling the photodiode output at 1 GS/s using an oscilloscope. An external reference signal, to which the graphene drum oscillator will be locked, is provided by a blue laser diode (2.5 mW, $\lambda = 405$ nm) whose intensity is electronically modulated.

Results and Discussion

Figure 1(b) shows the time-domain signals: the yellow trace indicates the free-running oscillator and the blue trace shows the output of the oscillator when the reference oscillator signal is applied. Figure 1(c) displays a zoom of the oscillations in more details. Figure 1(d) shows the power spectral densities (PSD) of the displacement signal, obtained by taking the FFT of the time traces. The spectral purity of the peak, given by its full-width at half-maximum (FWHM), is significantly better in the case with the reference signal (FWHM < 1 kHz) compared to the case without the reference signal (FWHM ≈ 35 kHz).

One would naively expect to see no slow phase dynamics beyond locking. Interestingly, the phase in both direct and parametric cases oscillates with a period of ~ 0.1 ms, shown in Fig. 2(a). To extract the frequency of the phase oscillations, a Lorentzian function is fitted to the PSD of the phase, as shown in the inset in Fig. 2(b). By fitting the PSD for the different drive powers at zero detuning, the dependence of the phase oscillation frequency on synchronization signal strength is obtained. Figure 2(b) shows these plotted on a logarithmic scale for both direct (blue) and parametric (red) entrainment. The frequency of the phase oscillation shows a power-law dependence on the strength of the reference signals. The exponents are $S_d = 0.56 \pm 0.18$ and $S_p = 0.61 \pm 0.03$, as obtained from the fits in Fig. 2(b). The slow phase oscillations and their power-dependence were reproduced qualitatively using a van der Pol-Duffing-Mathieu equation.

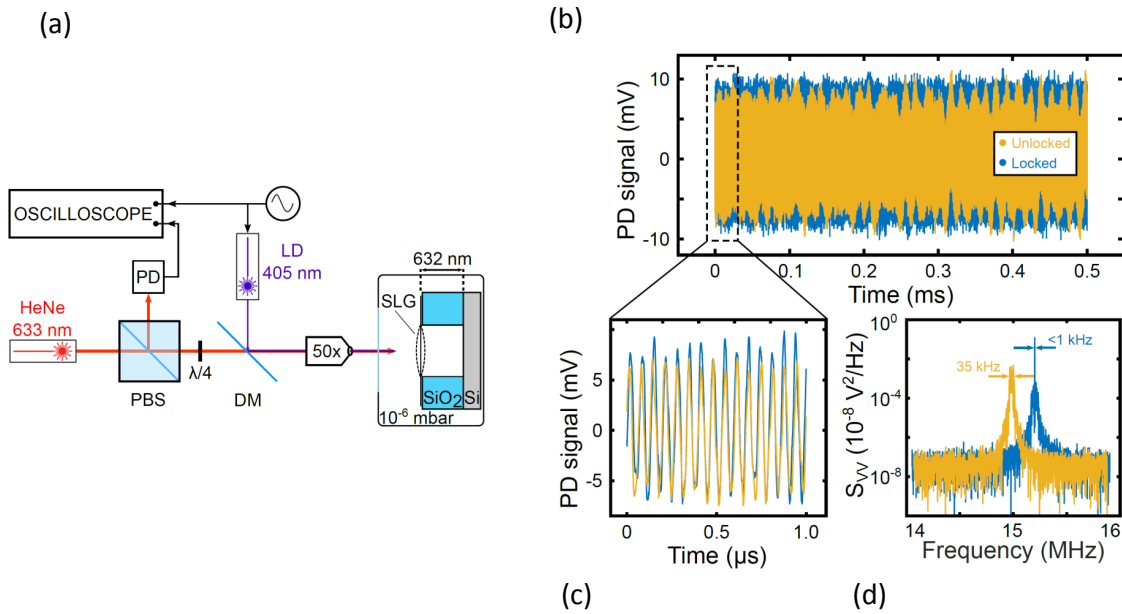


Figure 1: (a) Schematic representation of the measurement setup. A red He-Ne laser and a modulated blue laser are focused onto the drum via a window in the vacuum chamber of the cryostat at a temperature of 3 K. The displacement of the drum is detected using a photodiode (PD) and sampled with a digital oscilloscope. (b) A time-domain trace of the photodiode output for a free-running (yellow) and a synchronized (blue) oscillator. The frequency and power of the reference signal are $f_{\text{sync}} = 15.19$ MHz and a modulation strength of $P_d = 1.5$ mW respectively. (c) Zoom of the oscillation signal. (d) Power spectral density of the displacement and reference signals taken over a 1 ms time interval.

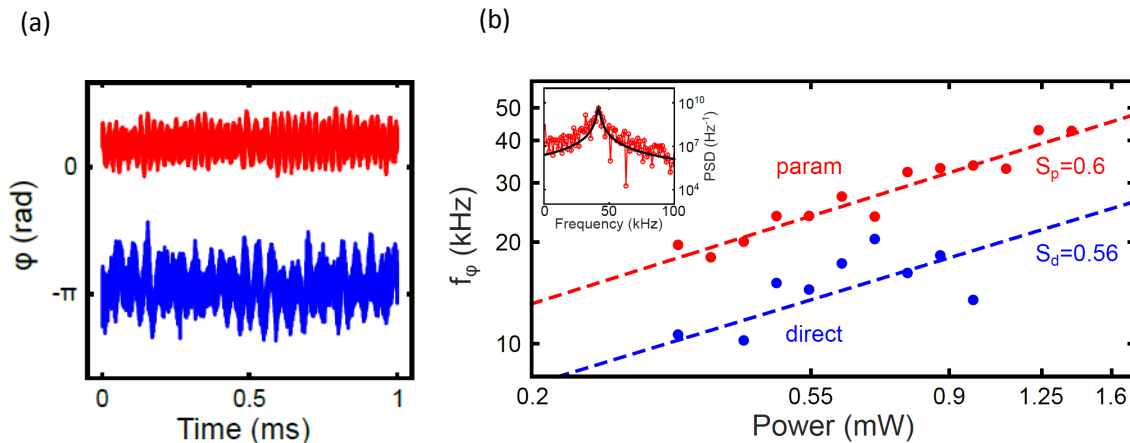


Figure 2: (a) Phase of the locked oscillator for the direct (blue) and parametric (red) entrainment. The locked phase also shows slow phase oscillations with a period of ~ 0.1 ms. (b) Experimental power-law dependence of the phase resonance frequency on signal strength (rms signal power) for direct (blue) and parametric (red) locking. Inset shows a PSD of the phase and a Lorentzian fit.

Conclusions

In summary, the current work demonstrates that graphene oscillators can be synchronized to both a direct and parametric external signal. It is shown that achieving entrainment can significantly reduce the width of the oscillation peak, thus allowing reduction of oscillator frequency fluctuations to produce stable nanoscale oscillating motion. In addition to phase-locking, we also observed phase resonance and found that its frequency exhibits a power-law dependence on the drive signal strength for both direct and parametric synchronization. These oscillations were qualitatively reproduced using a forced van der Pol-Duffing-Mathieu equation, with the Duffing nonlinearity playing a crucial role in making such behaviour possible. Potential applications of synchronized oscillators include optoelectronic modulators, sound generators and oscillating sensors.

References

- [1] Strogatz, S. H. (2003). Sync: How Order Emerges From Chaos In the Universe, Nature, and Daily Life. Hyperion.
- [2] Metzger, C. H., Karrai, K. (2004). Cavity cooling of a microlever. Nature, 432(7020), 1002-1005.
- [3] Metzger, C., Favero, I., Ortlieb, A., Karrai, K. (2008). Optical self cooling of a deformable Fabry-Perot cavity in the classical limit. Physical Review B, 78(3), 035309.
- [4] Barton, R. A., Storch, I. R., Adiga, V. P., Sakakibara, R., Cipriani, B. R., Ilic, B., Wang, S.P., Ong, P., McEuen, P.L., Parpia, J.M. and Craighead, H.G. (2012). Photothermal self-oscillation and laser cooling of graphene optomechanical systems. Nano letters, 12(9), 4681-4686.